

PRAME as an Independent Biomarker for Metastasis in Uveal Melanoma

Matthew G. Field¹, Christina L. Decatur¹, Stefan Kurtenbach¹, Gülçin Gezgin², Pieter A. van der Velden², Martine J. Jager², Kaleigh N. Kozak¹, and J. William Harbour¹

Abstract

Purpose: Uveal melanoma (UM) can be classified by gene expression profiling (GEP) into Class 1 (low metastatic risk) and Class 2 (high metastatic risk), the latter being strongly associated with mutational inactivation of the tumor suppressor *BAP1*. Nevertheless, a small percentage of Class 1 tumors give rise to metastatic disease. The purpose of this study was to identify biomarkers of metastasis in Class 1 tumors.

Experimental Design: A total of 389 consecutive patients with UM were assigned to Class 1 or Class 2 using a prospectively validated 12-gene prognostic classifier. Selected tumors were further analyzed using global GEP and single nucleotide polymorphism microarrays. *PRAME* (preferentially expressed antigen in melanoma) mRNA expression was analyzed in 64 Class 1 tumors by qPCR.

Results: Among Class 1 UMs, the most significant predictor of metastasis was *PRAME* mRNA expression ($P = 0.0006$). The 5-

year actuarial rate of metastasis was 0% for Class 1^{*PRAME*-}, 38% for Class 1^{*PRAME*+}, and 71% for Class 2 tumors. Median metastasis-free survival for Class 1^{*PRAME*+} patients was 88 months, compared to 32 months for Class 2 patients. Findings were validated using three independent datasets, including one using disomy 3 to identify low-risk UM. Chromosome copy number changes associated with Class 1^{*PRAME*+} tumors included gain of 1q, 6p, 8q, and 9q and loss of 6q and 11q. *PRAME* expression was associated with larger tumor diameter ($P = 0.05$) and *SF3B1* mutations ($P = 0.003$).

Conclusions: *PRAME* is an independent prognostic biomarker in UM, which identifies increased metastatic risk in patients with Class 1 or disomy 3 tumors. This finding may further enhance the accuracy of prognostic testing and precision medicine for UM. *Clin Cancer Res*; 22(5); 1234–42. ©2016 AACR.

Introduction

Uveal melanoma (UM) is the most common primary cancer of the eye and has a propensity for fatal hematogenous metastasis to the liver (1). The molecular landscape of primary UM has been well characterized (2). UMs can be categorized by gene expression profiling (GEP) into two molecular classes associated with metastatic risk: Class 1 (low metastatic risk) and Class 2 (high metastatic risk; ref. 3). Class 1 tumors retain a differentiated melanocytic phenotype and transcriptome, whereas Class 2 tumors have a dedifferentiated phenotype and stem cell-like transcriptome (4). The Class 2 signature is strongly associated with mutations in *BAP1* on chromosome 3p21, usually accompanied by loss of the other copy of chromosome 3, consistent with the "two hit" model of tumor suppressor gene inactivation (5, 6). Four other frequently mutated genes have been identified in UM. Hemizygous mutations in the G-protein subunits *GNAQ* and *GNA11* are early or initiating events in UM (7–9). *GNAQ* and *GNA11* mutations are mutually exclusive, and one or the other is found in ~83% of UMs (9). Hemizygous

mutations in *SF3B1* and *EIF1AX* are virtually mutually exclusive with each other, and with *BAP1* mutations, and they have been linked to good prognosis (10, 11).

GEP-based assignment of UMs to Class 1 or Class 2 with a 12-gene expression classifier has been validated in a prospective, multicenter study and is now routinely performed for clinical use in many centers (12, 13). Although the vast majority of UM metastases occur in patients with Class 2 tumors, a small proportion of Class 1 tumors also give rise to metastasis. Based on a retrospective analysis of expression data from the 12-gene classifier on Class 1 tumors that metastasized, a subgrouping of Class 1 tumors into "1A" and "1B" based on the expression of two of these genes (*CDH1* and *RAB31*) has been used as a provisional indicator of Class 1 patients who may be at increased risk of metastasis (14). Class 1A tumors have low *CDH1/RAB31* expression, and Class 1B tumors have high *CDH1/RAB31* expression. To identify additional and potentially more accurate biomarkers for metastasis in Class 1 tumors, we conducted a genome-wide integrated transcriptomic and chromosomal analysis in our cohort of Class 1 tumors. We identified the cancer-testis antigen *PRAME* (preferentially expressed antigen in melanoma) as a biomarker for increased metastatic risk in Class 1 tumors. This finding has important implications for precision management in patients with UM and may aid in the stratification of patients for clinical trials.

Materials and Methods

Clinical samples

This study was conducted with the approval of the Institutional Review Boards of Washington University and the University of

¹Bascom Palmer Eye Institute, Sylvester Comprehensive Cancer Center and Interdisciplinary Stem Cell Institute, University of Miami Miller School of Medicine, Miami, Florida. ²Department of Ophthalmology, Leiden University Medical Center, Leiden, The Netherlands.

Note: Supplementary data for this article are available at Clinical Cancer Research Online (<http://clincancerres.aacrjournals.org/>).

Corresponding Author: J. William Harbour, 900 NW 17th St, Miami, FL 33136. Phone: 305-326-6166; Fax: 305-326-6417; E-mail: harbour@miami.edu

doi: 10.1158/1078-0432.CCR-15-2071

©2016 American Association for Cancer Research.

Translational Relevance

Uveal melanoma (UM) can be stratified into Class 1 (low metastatic risk) and Class 2 (high metastatic risk) using a prospectively validated 12-gene expression profile. Although the vast majority of metastases occur in Class 2 tumors, a small percentage of Class 1 tumors also metastasize. This study revealed that metastasis in Class 1 tumors is strongly associated with expression of the *PRAME* oncogene. This finding was validated in three independent datasets, including one using disomy 3 as a surrogate marker for low risk UM. Adding *PRAME* to the 12-gene expression classifier will likely enhance its prognostic accuracy by identifying Class 1 tumors with intermediate metastatic risk. Some cancers expressing *PRAME* have been shown to be recognized by cytotoxic T cells, suggesting that immunotherapy may have a role in the precision management of patients with *PRAME*+ UM.

Miami. Tumor samples were obtained at enucleation or by fine needle biopsy between November 1998 and May 2015 from patients with UMs arising from the ciliary body and/or choroid. Samples were snap frozen and stored at -80°C . Baseline clinical information, metastatic status, and final outcome were recorded for each patient. Prognostic molecular class assignments (Class 1 or Class 2) were obtained using a prospectively validated 12-gene classifier as previously reported (13). Mutation status for *GNAQ*, *GNA11*, *BAP1*, *SF3B1*, and *EIF1AX* were obtained by Sanger sequencing as previously described (5, 7, 10, 11). Tumor samples from Leiden University were obtained between 1999 and 2008 by enucleation and clinical and histopathologic features were retrieved from patient charts and histology reports. Data on survival were obtained from medical records and the Integral Cancer Center West, which updates patient follow-up information, including date and cause of death, on a yearly basis. Under Dutch law, tumor material may be used for research purposes, and patients signed an informed consent for genetic testing. The tenets of the Declaration of Helsinki were followed in all studies.

RNA expression analysis

Total RNA was isolated using TRIzol and the Qiagen RNeasy Kit. RNA quality was assessed on the Agilent Bioanalyzer 2100. RNA from enucleated samples was hybridized to Illumina Human HT12v4 BeadChip arrays, and resulting data have been deposited in the NCBI's Gene Expression Omnibus (15) and are accessible through GEO Series accession number GSE73652. Raw data were normalized by cubic spline using Illumina GenomeStudio. Significance Analysis of Microarrays (SAM version 4.0) was used to generate a ranked list of differentially expressed genes based on false discovery rate and fold change (16). Gene Set Enrichment Analysis (GSEA version 2.0.4) was used to identify significantly enriched functional gene sets (17). Differentially upregulated and downregulated genes from SAM were input into GSEA and analyzed using the Molecular Signatures Database (MSigDB) to identify chromosomal position and transcription factor target gene sets. A circular plot of gene expression data was generated using the Perl-based Circos graphical program (18). Expression data of specific chromosomal regions were plotted using the R package *GViz*. Principal component analysis (PCA) and three-

dimensional (3D) visualization using the 12-gene expression classifier were performed using Partek Genomics Suite. Unsupervised PCA and 3D visualization using global transcriptomic data were performed on the top 20% most variable genes across all samples using the *stats* and *rgl* packages in R.

PRAME mRNA expression was analyzed using real-time quantitative PCR (qPCR). RNA was converted to cDNA using the Applied Biosystems High Capacity cDNA Reverse Transcription Kit, and gene expression was quantified using the Applied Biosystems 7900HT Real-Time PCR System with TaqMan primers and Gene Expression Master Mix following the manufacturer's protocol. The control genes for the 12-gene expression classifier (*MRPS21*, *RBM23*, and *SAPI30*) were included. TaqMan primers were Hs01022301_m1 (*PRAME*), Hs00230458_m1 (*MRPS21*), Hs00216503_m1 (*RBM23*), and Hs00368617_m1 (*SAPI30*). Ct values were calculated using the manufacturer's software, and mean Ct values were calculated for all triplicate sets. ΔCt values were calculated by subtracting the mean Ct of each discriminating gene from the geometric mean of the mean Ct values of the three endogenous control genes, as previously described (19).

For Kaplan–Meier actuarial analysis, *PRAME* mRNA expression data were scaled from 0 to 1 and plotted from lowest to highest expression. A Loess model was constructed to represent the best fit of the data (second degree, span = 0.5, family = Gaussian, fitting by least-squares), and the differences in predicted values of the Loess model were plotted to estimate slope change (Supplementary Fig. S1A). Samples with minimal differences (blue dots) were coded as *PRAME*–, whereas those with significant differences (red dots) were coded as *PRAME*+.

For validation, three independent gene expression datasets and associated clinical annotations were analyzed. Two of these datasets were obtained from GEO (15), and tumor samples were stratified into Class 1 or Class 2 based on the 12-genes in the UM classifier. Dataset #GSE22138 was performed on the Affymetrix Human Genome U133 Plus 2.0 Array platform and dataset #GSE44295 was performed on the Illumina Ref8 platform. These datasets consisted of 20 Class1^{*PRAME*–} and 31 Class1^{*PRAME*+} tumors. The third dataset contained 25 tumors classified as low risk based on disomy 3, which is significantly associated with the Class 1 signature (6, 13), and was performed at Leiden University on the Illumina Human HT12v4 BeadChip Array platform. For these additional datasets, *PRAME* gene expression was scaled from 0 to 1 for all samples and categorized as *PRAME*+ or *PRAME*–, as described above.

Immunohistochemistry

Immunohistochemistry (IHC) for *PRAME* was performed with the SIGMA Prestige anti-*PRAME* antibody (HPA045153) at 4 $\mu\text{g}/\text{mL}$ on formalin-fixed, paraffin-embedded (FFPE) slides using the VECTASTAIN UNIVERSAL Elite ABC Kit (Vector Laboratories, PK-6200) and the ImmPACT SG Peroxidase Substrate Kit (Vector Laboratories, SK-4705) according to the manufacturer's recommendation, with the following changes. Primary antibody was incubated overnight at 4°C with addition of 0.3% Triton X-100. Antigen retrieval was performed in sodium citrate buffer (10 mmol/L, 0.05% Tween 20, pH 6.0) in an autoclave at 121°C for 10 minutes. Slides were slowly cooled down to 80°C for 25 minutes, and additionally for 10 minutes at room temperature. The blocking step was changed to 1 hour. Incubation with secondary antibody was increased to 1 hour with addition of 0.1% Triton X-100. Incubation with VECTASTAIN Elite ABC

reagent was increased to 1 hour. ImmPACT SG reagent was applied for 20 minutes, with changing to fresh substrate after 7 and 14 minutes. Nuclear fast red counter-stain (Vector Laboratories, H-3403) was applied for 10 minutes. Negative controls included tumors known to be lacking *PRAME* mRNA expression and samples tested with secondary antibody only. Two independent investigators assessed the IHC slides for *PRAME* nuclear staining in a blinded manner. Samples were graded by the percentage of cells demonstrating nuclear staining. The scores from the independent graders were averaged.

Chromosome copy number analysis

Genomic DNA was isolated using the Qiagen DNeasy Kit. For the Class1^{met+} samples, loss of heterozygosity for chromosome 3 was determined using a single nucleotide polymorphism (SNP) assay as previously described (20). For *PRAME*+ and *PRAME*- samples, SNP analysis was performed using the Affymetrix Genome-Wide Human SNP 6.0 array and data were analyzed for copy number gains and losses as described in the Affymetrix Genotyping Console software user manual and then plotted with Integrative Genomics Viewer. For the Leiden dataset, monosomy 3 was determined using Affymetrix 250K_SNP and Cytoscan HD microarrays as previously described with a cut-off value of <1.9 for chromosomal loss (6).

Statistical analysis

Statistical analysis was determined using Medcalc version 14.10.2. Statistical significance was determined using the Mann-Whitney test for continuous variables, Fisher exact test for discrete variables, Cox proportional hazards regression for evaluation of prognostic factors for survival, Spearman rank correlation coefficient for comparison of continuous nonparametric data, and Kaplan-Meier method with log-rank test and right censoring for comparing survival between groups.

Results

Clinical characteristics of metastasizing Class 1 UMs

Our study design is summarized in Supplementary Table S1. Among 389 consecutive patients with UM involving the ciliary body and/or choroid who underwent GEP prognostic testing, the molecular class assignment was Class 1 in 216 (56%) patients and Class 2 in 173 (44%) patients. Class 2 GEP was associated with markedly greater metastatic risk than Class 1 GEP, with metastatic disease being detected in 12/216 (6%) Class 1 cases versus 63/173 (36%) Class 2 cases (log rank test, $P < 0.0001$; Supplementary Fig. S1B).

We wished to determine whether any clinicopathologic features differed between Class 1 tumors with metastasis (Class1^{met+}) and Class 2 tumors with metastasis (Class2^{met+}). Class2^{met-} tumors were not included in this analysis because the high metastatic rate and limited follow-up in some cases would have led to the erroneous inclusion of tumors that would later metastasize. Pairwise comparisons of clinicopathologic features are summarized in Supplementary Table S2. Detailed clinicopathologic and molecular features of all the Class1^{met+} tumors are summarized in Supplementary Table S3. Among 52 patients in whom metastasis was detected and the sites of metastasis were available, the liver was affected in 6/12 (50%) patients with a Class1^{met+} tumor compared to 36/40 (90%) patients with a Class2^{met+} tumor (Fisher exact test, $P = 0.02$). Other metastatic

sites in Class 1 tumors included lung in 4, bone in 3, and stomach in 2 cases. Compared to Class2^{met+} tumors, Class1^{met+} tumors were associated with younger patient age and less frequent ciliary body involvement (Mann-Whitney test, $P = 0.04$ and 0.02 , respectively).

Similarly, we compared the characteristics of the Class 1 tumors with and without metastatic disease. Pairwise comparisons of clinicopathologic features are summarized in Supplementary Table S2. There were no significant differences between Class1^{met+} and Class1^{met-} tumors with regard to age, sex, tumor diameter or thickness, ciliary body involvement, or cell type. For Class1^{met+} tumors, mutations were identified in *BAP1* in none of eight, *EIF1AX* in none of six, *GNAQ* in five of eight, *GNA11* in one of seven, and *SF3B1* in four of eight samples in which DNA was still available for sequencing (Supplementary Table S3).

Comparison of gene expression profiles among Class 1 tumors

Among the five known UM driver mutations, *SF3B1* mutations were most strongly associated with Class 1 metastasis, but because these mutations were only present in 50% of metastatic cases, it is not an adequate biomarker for Class 1 metastasis. Thus, we turned to transcriptomic profiling. Initially, we analyzed 108 Class 1 tumors by PCA using the mRNA expression of genes from the 12-gene classifier. PCA organized the samples into two clusters corresponding to their metastatic status (Supplementary Fig. S1C), indicating that there were potentially meaningful transcriptomic differences between Class1^{met+} and Class1^{met-} tumors. To identify genes that were differentially expressed between Class1^{met+} and Class1^{met-} tumors, we performed a genome-wide transcriptomic analysis of five Class1^{met+} tumors and eight Class1^{met-} tumors with at least 1 year of follow-up using the Illumina Human HT12v4 Expression BeadChip array. Using SAM, differentially expressed genes were identified at a significance level of FDR <0.01 (Fig. 1A and Supplementary Table S4). Using unsupervised PCA, tumor samples once again clustered into two distinct groups that corresponded to their metastatic status, with no overlap in their 95% confidence ellipsoids (Fig. 1B). By far, the most highly overexpressed gene in Class1^{met+} tumors was *PRAME* (Mann-Whitney test, $P = 0.003$; Fig. 1C-D).

We then analyzed *PRAME* expression by qPCR in 26 Class 1 tumors, 7 with metastasis and 19 without metastasis with even longer follow-up of >3 years. These samples included 17 that were not previously analyzed. Consistent with the array data, 16/19 (84%) Class1^{met-} tumors showed minimal *PRAME* expression (Class1^{PRAME-}), whereas 7/7 (100%) of Class1^{met+} tumors showed elevated *PRAME* expression (Class1^{PRAME+}, Mann-Whitney test, $P = 0.001$; Fig. 1E). We performed IHC for *PRAME* protein on 6 of the Class 1 tumors in which original FFPE blocks were still available, and as expected, *PRAME* mRNA expression correlated with nuclear protein expression (Fig. 1F and Supplementary Fig. S1D). There was no significant association between *PRAME* expression status and the currently used Class "1A/1B" designation (Mann-Whitney test, $P = 0.5$; Fig. 1G). However, among Class 1 tumors in which both *PRAME* and 1A/1B data were available, all six Class 1 tumors that metastasized were *PRAME*+ and Class 1B.

To obtain a more accurate assessment of the prevalence of *PRAME*-expressing Class 1 tumors, and to obtain actuarial estimates of metastatic risk associated with *PRAME* expression in Class 1 tumors, we performed qPCR on an additional 38 samples, for a total of 64 Class 1 tumors analyzed by qPCR. The overall

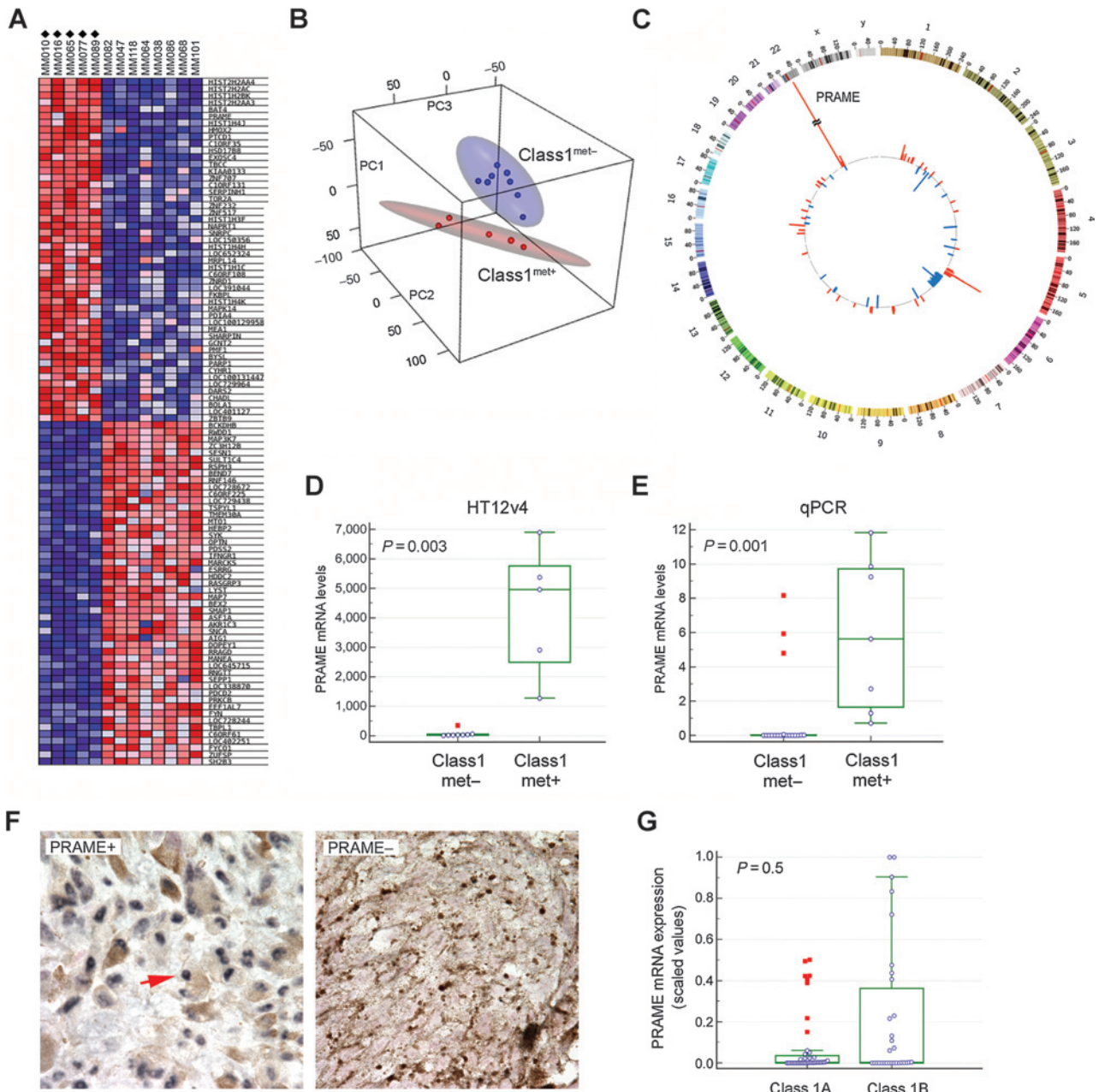
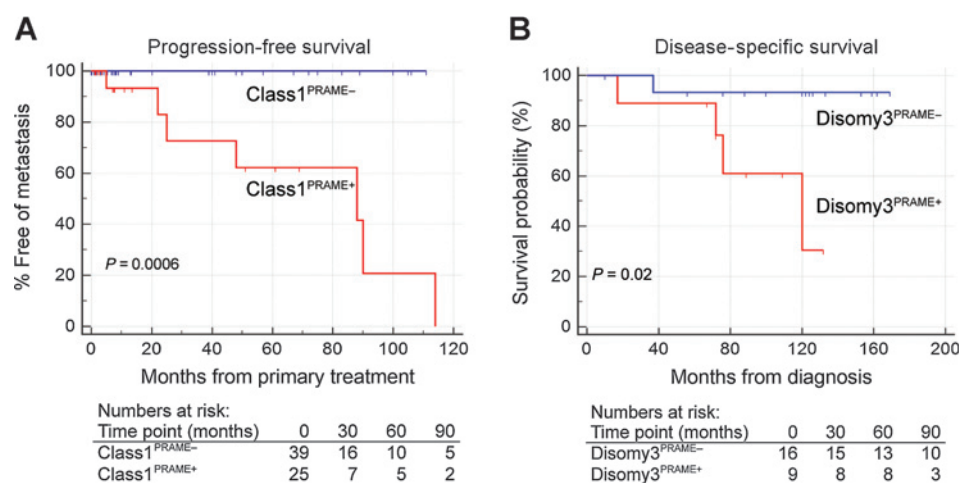


Figure 1. Gene expression profiling of Class 1 primary uveal melanomas (UMs) based on metastatic status. A, heatmap showing the 50 most highly upregulated and downregulated genes in five Class 1 primary UMs that metastasized (Class1^{met+} tumors, indicated by diamonds) versus eight that did not (Class1^{met-} tumors). Gene expression profiles were obtained using Illumina Human HT12v4 BeadChip arrays and analyzed with significance analysis of microarrays (SAM). Blue = decreased gene expression, red = increased gene expression in Class1^{met+} versus Class1^{met-} tumors. B, unsupervised principal component analysis of the same dataset, showing differential clustering of Class1^{met+} (red) and Class1^{met-} (blue) tumors. Red and blue ellipsoids represent 95% confidence intervals for each respective group. C, circos plot of the same dataset demonstrating genes that are significantly upregulated (red) or downregulated (blue) in Class1^{met+} compared to Class1^{met-} tumors with respect to chromosomal location. D, Box-and-whisker plots of *PRAME* mRNA expression in Class1^{met+} versus Class1^{met-} tumors ≥ 1 year of follow-up using the Illumina Human HT12v4 BeadChip array dataset. E, box-and-whisker plots of *PRAME* mRNA expression in Class1^{met+} versus Class1^{met-} tumors with ≥ 3 years of follow-up using qPCR. F, representative examples of immunohistochemical staining for PRAME in Class1^{PRAME+} and Class1^{PRAME-} tumors, 100 \times magnification. Blue, PRAME nuclear staining (arrow); brown, intrinsic melanin pigment; red, nuclear counterstain. G, analysis of *PRAME* mRNA expression with respect to Class 1A versus Class 1B designation. In box-and-whiskers plots, the central box represents the 25th to 75th percentiles, the middle line represents the median, the horizontal bars represent the minimum and maximum values, except for "far out" values, indicated by red boxes and defined as values larger than the upper 75% plus three times the interquartile range.

median follow-up was 8.2 months (mean 31.5 months, interquartile range 3.3–57.1 months). Using the stratification procedure described in Materials and Methods, 39 (61%) tumors were

categorized as Class1^{PRAME-} and 25 (39%) as Class1^{PRAME+}. Using Kaplan–Meier survival analysis, *PRAME* status was strongly associated with metastasis (log rank test, $P = 0.0006$). Indeed, no

Downloaded from <http://aacrjournals.org/clincancerres/article-pdf/22/5/1234/203937/1234.pdf> by guest on 19 May 2023

**Figure 2.**

Survival analysis in patients with Class 1 primary uveal melanoma (UM). A, Kaplan-Meier plot showing metastasis-free survival in 39 patients with Class1^{PRAME-} (blue) and 25 patients with Class1^{PRAME+} (red) UMs. B, Kaplan-Meier plot showing metastasis-free survival in 16 patients with Disomy3^{PRAME-} (blue) and 9 patients with Disomy3^{PRAME+} (red) UMs.

metastatic events occurred among Class1^{PRAME-} cases (Fig. 2A). The 5-year actuarial probability of metastasis was 15% for Class 1 tumors overall, 0% for Class1^{PRAME-} tumors and 38% for Class1^{PRAME+} tumors, compared to 71% for Class 2 tumors. The median metastasis-free survival for patients with Class1^{PRAME+} tumors was 88 months, compared to 32 months for Class 2 tumors. *PRAME* expression showed a significant association with larger basal tumor diameter (Spearman correlation, $P = 0.04$) and with *SF3B1* mutations (Mann-Whitney test, $P = 0.003$; Supplementary Fig. S1E).

To further validate the association of high *PRAME* levels with metastasis, we combined two independent published datasets with long follow-up (GSE22138 and GSE44295), which included 20 Class1^{PRAME-} and 31 Class1^{PRAME+} cases (median follow-up 68.0 months, mean 80.4 months, interquartile range 41.4–101.5 months). By Kaplan-Meier survival analysis, *PRAME* expression was significantly associated with metastasis (log rank test, $P = 0.05$; Supplementary Fig. S1F). The 5-year actuarial probability of metastasis was very similar to our dataset: 21% for Class 1 tumors overall, 5% for Class1^{PRAME-} tumors, and 31% for Class1^{PRAME+} tumors.

We analyzed a third dataset with long follow-up from Leiden University that defined low risk UM by the presence of disomy 3. This dataset of 64 cases included 16 Disomy3^{PRAME-} tumors and 9 Disomy3^{PRAME+} tumors, with a median follow-up of 121.0 months (mean, 107.7 months; interquartile range, 85.0–138.0 months) and 76.0 months (mean, 83.8 months; interquartile range, 72.0–109.0 months), respectively. Comparable to the other datasets, *PRAME* expression in these tumors was associated with increased metastatic risk (log rank test, $P = 0.02$; Fig. 2B). Similar to our previous findings, *PRAME* expression in these tumors was associated with larger basal tumor diameter ($P = 0.001$).

Functional analysis of the Class1^{PRAME+} transcriptome

Genes that were differentially expressed between Class1^{PRAME-} and Class1^{PRAME+} tumors were analyzed for chromosomal location, biologic function, and transcription factor binding sites using GSEA and MSigDB to gain insights into tumor biology. Genes that were upregulated in Class1^{PRAME+} tumors showed a significant enrichment in chromosomal location at 1q21, 1q42, 6p21-22, and 8q24, whereas downregulated genes showed

enrichment across most of chromosome 6q (FDR < 0.01 for all; Supplementary Table S5). At FDR = 0.02, enrichment of down-regulated genes was also observed at 11q23-24.

Genes that were upregulated in Class1^{PRAME+} tumors were also enriched for biologic functions related to chromosome maintenance, DNA replication, and base excision repair (FDR ≤ 0.2 for all; Fig. 3A and Supplementary Table S6). Analysis of genes upregulated in Class1^{PRAME+} tumors for transcription factor binding sites within the promoter region (±2 kb of the transcription start site) showed enrichment for two known transcription factors: NFY and SP1 (FDR < 0.01 for both; Supplementary Table S5). Interestingly, *PRAME* associates with NFY at its CCAAT binding site in promoter regions to induce transcriptional activation (21), and many of the upregulated genes with NFY sites in their promoters were located within regions of chromosomal gain on 1q and 6p in Class1^{PRAME+} tumors (Supplementary Fig. S2).

Chromosomal alterations in Class1^{PRAME+} tumors

The correlation between mRNA expression of *PRAME* and of genes involved in chromosome maintenance suggested that Class1^{PRAME+} tumors may demonstrate increased chromosomal gains and losses relative to Class1^{PRAME-} tumors. To test this hypothesis, we used high-density Affymetrix Genome-Wide Human SNP 6.0 arrays to analyze nine Class1^{PRAME+} tumors (six with metastasis and three without metastasis) and four Class1^{PRAME-} tumors (all without metastasis). Indeed, there was a correlation between *PRAME* expression and specific chromosomal gains and losses, even in this limited set of cases (Fig. 3B). Consistent with our transcriptomic analysis (Supplementary Table S5), the most common chromosome copy number changes specific to Class1^{PRAME+} tumors included 1q gain (five cases, all with metastasis), 6p gain with 6q loss (five cases, all with metastasis), and 8q gain (eight cases, six with metastasis and two without metastasis). Less common but potentially important changes that were specific to Class1^{PRAME+} tumors included 9q gain (three cases, all with metastasis) and 11q loss (four cases, three with metastasis and one without metastasis). 6p gain was only specific to Class1^{PRAME+} tumors when accompanied by 6q loss, consistent with isochromosome 6p (22). In the Leiden dataset, gain or amplification of 8q was observed in 6/16 Disomy3^{PRAME-} and in 8/9 Disomy3^{PRAME+} tumors (Fisher exact

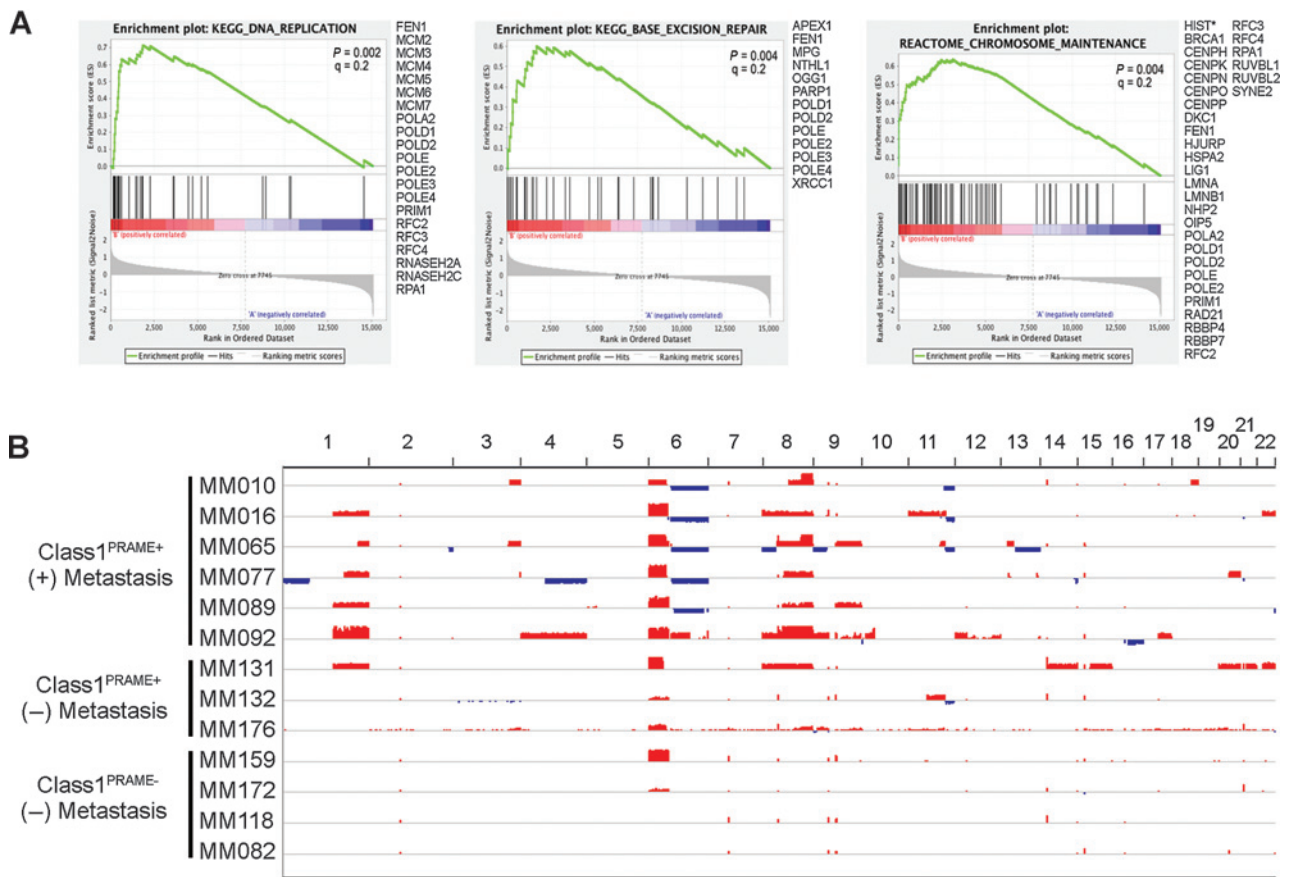


Figure 3. Functional and chromosome copy number analyses in Class 1 primary uveal melanoma (UM). A, gene set enrichment analysis (GSEA) of annotated gene sets exhibiting significant enrichment for genes that were upregulated in Class1^{PRAME+} tumors relative to Class1^{PRAME-} tumors. B, high-density Affymetrix Genome-Wide Human SNP 6.0 Array analysis of Class1^{PRAME+} and Class1^{PRAME-} tumors with respect to metastatic status. Blue indicates copy number loss, and red, copy number gain.

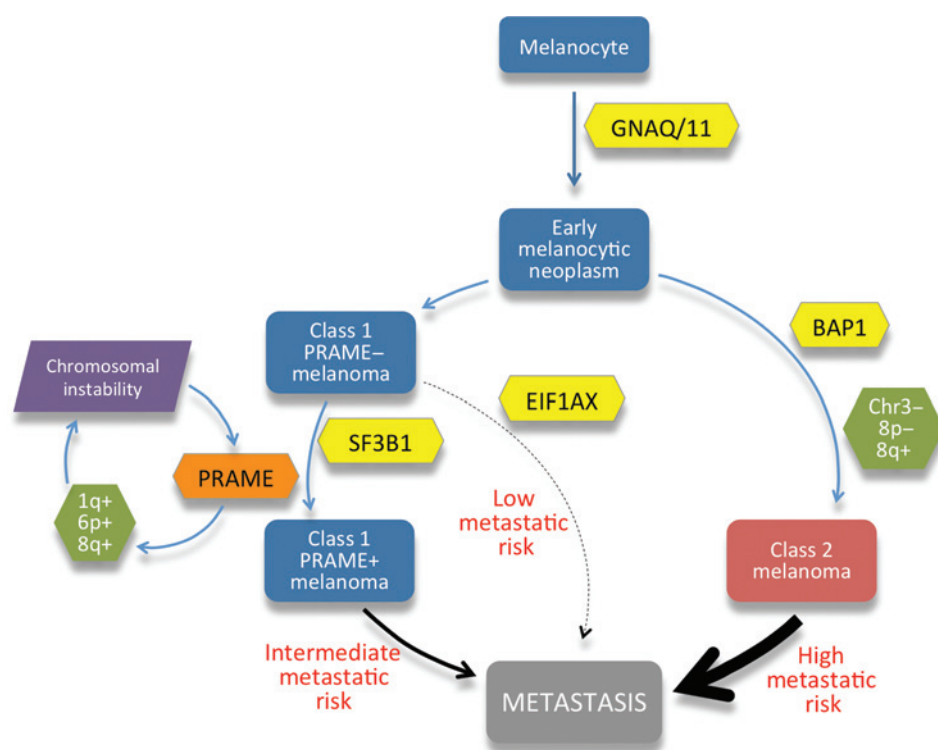
test, $P = 0.03$). Although chromosome 6 status did not show a significant difference between Disomy3^{PRAME-} and Disomy3^{PRAME+} tumors (data not shown), 8/9 Disomy3^{PRAME+} tumors displayed a gain of 6p. We elected not to pursue further chromosomal analyses because *PRAME* met our objective for this study, which was to identify a strong biomarker for Class 1 metastasis.

Discussion

The clinical and molecular features associated with metastasis in Class 1 tumors were clearly distinct from those associated with metastasis in Class 2 tumors. Class 1 UMs that metastasized tended to occur in younger patients, less frequently involved the ciliary body, less frequently metastasized to the liver, lacked *BAP1* mutations, frequently had *SF3B1* mutations, and exhibited a distinct GEP. The transcriptomes of Class 1 and Class 2 tumors were so dramatically different that the comparatively subtle differences between Class1^{met-} and Class1^{met+} were masked until Class 2 tumors were first removed from the analysis. When this was done, however, the gene expression differences between these Class 1 subgroups were clearly evident, and *PRAME* was the single most differentially expressed gene that distinguished Class 1

tumors based on their metastatic status. When we expanded the analysis to a larger number of tumor samples and stratified the tumors based on the presence or absence of *PRAME* expression measured by qPCR, Kaplan–Meier survival analysis confirmed the strong association of *PRAME* with metastasis in Class 1 tumors. This finding was validated in three independent datasets, including one that used disomy 3 to define "low risk" UM. As expected, we also found that *PRAME* mRNA expression correlated with *PRAME* nuclear protein expression by IHC. A rigorous analysis of *PRAME* IHC staining was beyond the scope of this study but needs to be performed in a large number of FFPE samples to confirm whether this has similar prognostic value as *PRAME* mRNA expression.

The 12-gene classifier is a prospectively validated clinical prognostic test for UM (13), and we anticipate that the addition of *PRAME* will further enhance the classifier's accuracy. There was no significant correlation between *PRAME* status and the provisional "1A/1B" system that the classifier currently uses. As such, we are initiating a multicenter study to compare these two predictors, and we anticipate that *PRAME* will likely be the more accurate biomarker for metastasis in Class 1 UMs because it was identified in an unsupervised manner from a global genomic analysis and was independently validated.

**Figure 4.**

Molecular hypothesis of tumor progression in UM, highlighting the role of PRAME reported herein. Increased PRAME mRNA expression in Class 1 UMs is associated with transcriptional upregulation of key genes involved in chromosome maintenance and stability, many of which are located on chromosome 1q and 6p and contain regulatory elements for transcription factors that interact with PRAME, including the retinoic acid receptor and NFY complexes. These observations suggest a possible feed-forward mechanism in which progressively increasing PRAME expression and specific chromosomal gains mutually reinforce one another to promote Class 1 tumor progression. There was a significant association of this pathway with *SF3B1* mutations, which were mutually exclusive with *EIF1AX* mutations, suggesting a bifurcated pathway. This Class 1 metastatic pathway was distinct from the more common pathway leading to metastasis through the bi-allelic loss of *BAP1* and acquisition of the Class 2 gene expression profile.

PRAME was initially discovered as a tumor antigen recognized by cytolytic T cells in cutaneous melanoma (23). PRAME expression is a marker of poor clinical outcome in a variety of cancers (24), and PRAME mRNA expression was recently found to be an important biomarker for differentiating benign nevi from malignant melanoma of the skin (25). PRAME may promote tumor progression, at least in part, by inhibiting differentiation, growth arrest, and apoptosis induced by retinoic acid signaling (26). PRAME binds the retinoic acid receptor (RAR) and recruits EZH2 to form a heterotrimeric complex that represses transcription of genes containing RAR binding sites. Consistent with the possibility that PRAME may inhibit retinoic acid signaling in Class1^{PRAME+} tumors, we found that 16% of genes downregulated in Class1^{PRAME+} tumors had a retinoic acid response element within ± 10 Kb of the transcription start site or gene end, including *RARB* itself (FDR ≤ 0.05 ; Supplementary Table S5). The cooperation between PRAME, RAR, and EZH2 suggests a potential therapeutic role for EZH2 inhibitors in patients with metastatic Class 1 tumors (27), particularly because EZH2 has been shown to repress immune signaling in UM cells (28). In addition, combination therapy with retinoic acid and an HDAC inhibitor may have therapeutic benefit by synergistically inhibiting PRAME to induce differentiation and cell-cycle exit (29). Interestingly, UM cells treated with retinoic acid become sensitive to killing by cytolytic T cells and NK cells (30), suggesting a potential role for immunotherapy in Class 1 metastasis. Vaccines against PRAME in cutaneous melanoma and other cancers are currently in clinical trials (trial nos. NCT01149343 and NCT01853878), and other immunotherapies directed against PRAME-expressing cancers are in development (31).

PRAME also associates with the transcription factor NFY at transcriptionally active promoters and enhancers containing the NFY binding motif CCAAT (21). NFY is a highly conserved, sequence-specific, nucleosome-like, trimeric complex that interacts with DNA in a sequence-specific manner (32). Although PRAME does not directly bind to NFY, its association at the NFY CCAAT binding motif is required for NFY-mediated transcriptional activation, whereas lack of PRAME is associated with repression (21). Intriguingly, many of the genes that were upregulated in Class1^{PRAME+} tumors contain NFY sites in their promoter and are located within the regions of 1q and 6p gain in Class1^{PRAME+} tumors. Furthermore, many of these genes play a role in meiotic recombination, telomere and chromosome maintenance, DNA replication, and base excision repair, all of which have been implicated in chromosomal instability (33). Moreover, NFYA, the component of the NFY trimeric complex that contains the CCAAT DNA-binding motif, is also located on 6p, and is significantly upregulated (FDR < 0.05). These findings suggest that PRAME upregulation may cooperate with copy number gains on 1q and 6p to facilitate chromosomal instability associated with tumor progression (Fig. 4).

Mutations in *SF3B1* and *EIF1AX* are associated with Class 1 GEP and have been reported to be good prognostic factors in UM, whereas *BAP1* mutations are associated with Class 2 GEP and poor prognosis (10, 11). Although this study affirms that *SF3B1* mutations are associated with better prognosis than *BAP1* mutations, we found that *SF3B1* mutations were associated with increased metastatic risk among Class 1 tumors, which almost never have *BAP1* mutations. Similarly, another group recently reported that patients with disomy 3 have a

worse disease-free survival when an *SF3B1* mutation is present (34). In the same way, 6p gain is a good prognostic factor relative to Class 2 GEP (and monosomy 3), 6p gain should not be thought of as "protective" against metastasis because it is strongly associated with metastasis in Class 1 tumors. However, *EIF1AX* mutations were not found in any of the metastasizing Class 1 tumors and were almost always mutually exclusive with *SF3B1* and *BAP1* mutations, suggesting that this mutation may have value as a favorable prognostic factor. Larger numbers of cases will need to be evaluated to determine the prognostic value of these mutations.

A limitation of this study was the small number of Class 1^{met+} cases, but this is a reflection of the infrequency of metastasis in Class 1 tumors. To overcome this limitation, we validated the prognostic significance of *PRAME* in three independent datasets, which all had long (> 6 years) median follow-up data. Furthermore, we are planning a prospective, multicenter study to validate these findings, establish the optimal *PRAME* expression threshold for maximizing positive and negative predictive value, and determine whether *PRAME* has prognostic value in Class 2 tumors. It is possible that some Class 1^{met-} tumors might have metastasized if they had been followed for a longer period of time. Indeed, rare metastatic events can occur even decades after primary ocular treatment (35). However, it is difficult to obtain such long-term data, and our findings are of practical value for the vast majority of patients for whom 5-year outcome projections are most important for personal and clinical decision-making.

For Class 1 tumors, the inclusion of *PRAME* expression may further augment the prognostic accuracy of the clinically available 12-gene classifier for UM. This finding allows patients with UM to be stratified into Class 1^{PRAME-} (low metastatic risk), Class 1^{PRAME+} (intermediate metastatic risk) and Class 2 (high metastatic risk) for purposes of metastatic surveillance and clinical trials of targeted adjuvant therapies.

References

- Ramaiya KJ, Harbour JW. Current management of uveal melanoma. *Exp Rev Ophthalmol* 2007;2:939-46.
- Harbour JW, Chao DL. A molecular revolution in uveal melanoma: implications for patient care and targeted therapy. *Ophthalmology* 2014;121:1281-8.
- Onken MD, Worley LA, Ehlers JP, Harbour JW. Gene expression profiling in uveal melanoma reveals two molecular classes and predicts metastatic death. *Cancer Res* 2004;64:7205-9.
- Chang SH, Worley LA, Onken MD, Harbour JW. Prognostic biomarkers in uveal melanoma: evidence for a stem cell-like phenotype associated with metastasis. *Melanoma Res* 2008;18:191-200.
- Harbour JW, Onken MD, Roberson ED, Duan S, Cao L, Worley LA, et al. Frequent mutation of *BAP1* in metastasizing uveal melanomas. *Science* 2010;330:1410-3.
- van Essen TH, van Pelt SI, Versluis M, Bronkhorst IH, van Duinen SG, Marinkovic M, et al. Prognostic parameters in uveal melanoma and their association with *BAP1* expression. *Br J Ophthalmol* 2014;98:1738-43.
- Onken MD, Worley LA, Long MD, Duan S, Council ML, Bowcock AM, et al. Oncogenic mutations in *GNAQ* occur early in uveal melanoma. *Invest Ophthalmol Vis Sci* 2008;49:5230-4.
- Van Raamsdonk CD, Bezroukove V, Green G, Bauer J, Gaugler L, O'Brien JM, et al. Frequent somatic mutations of *GNAQ* in uveal melanoma and blue naevi. *Nature* 2009;457:599-602.
- Van Raamsdonk CD, Griewank KG, Crosby MB, Garrido MC, Vemula S, Wiesner T, et al. Mutations in *GNA11* in uveal melanoma. *N Engl J Med* 2010;363:2191-9.
- Harbour JW, Roberson ED, Anbunathan H, Onken MD, Worley LA, Bowcock AM. Recurrent mutations at codon 625 of the splicing factor *SF3B1* in uveal melanoma. *Nat Genet* 2013;45:133-5.
- Martin M, Masshoffer L, Temming P, Rahmann S, Metz C, Bornfeld N, et al. Exome sequencing identifies recurrent somatic mutations in *EIF1AX* and *SF3B1* in uveal melanoma with disomy 3. *Nat Genet* 2013;45:933-6.
- Onken MD, Worley LA, Tuscan MD, Harbour JW. An accurate, clinically feasible multi-gene expression assay for predicting metastasis in uveal melanoma. *J Mol Diagn* 2010;12:461-8.
- Onken MD, Worley LA, Char DH, Augsburger JJ, Correa ZM, Nudleman E, et al. Collaborative Ocular Oncology Group report number 1: prospective validation of a multi-gene prognostic assay in uveal melanoma. *Ophthalmology* 2012;119:1596-603.
- Castle Biosciences Inc. [Internet]. DecisionDx-UM Summary. c2015 [cited 2014 December 10]; Available from: <http://www.myuvealmelanoma.com/health-care-professionals/decisiondx-um-summary/>
- Barrett T, Wilhite SE, Ledoux P, Evangelista C, Kim IF, Tomashevsky M, et al. NCBI GEO: archive for functional genomics data sets—update. *Nucleic Acids Res* 2013;41:D991-5.
- Tusher VG, Tibshirani R, Chu G. Significance analysis of microarrays applied to the ionizing radiation response. *Proc Natl Acad Sci U S A* 2001;98:5116-21.
- Subramanian A, Tamayo P, Mootha VK, Mukherjee S, Ebert BL, Gillette MA, et al. Gene set enrichment analysis: a knowledge-based approach for interpreting genome-wide expression profiles. *Proc Natl Acad Sci U S A* 2005;102:15545-50.

Disclosure of Potential Conflicts of Interest

J.W. Harbour is the inventor of intellectual property used in the study and receives royalties from its commercialization. He is a paid consultant for Castle Biosciences, licensee of intellectual property presented in this article. No potential conflicts of interest were disclosed by the other authors.

Authors' Contributions

Conception and design: J.W. Harbour

Development of methodology: S. Kurtenbach, J.W. Harbour

Acquisition of data (provided animals, acquired and managed patients, provided facilities, etc.): M.G. Field, C.L. Decatur, S. Kurtenbach, G. Gezgin, P.A. van der Velden, M.J. Jager, K.N. Kozak

Analysis and interpretation of data (e.g., statistical analysis, biostatistics, computational analysis): M.G. Field, S. Kurtenbach, G. Gezgin, M.J. Jager, K.N. Kozak, J.W. Harbour

Writing, review, and/or revision of the manuscript: M.G. Field, S. Kurtenbach, G. Gezgin, M.J. Jager, K.N. Kozak, J.W. Harbour

Administrative, technical, or material support (i.e., reporting or organizing data, constructing databases): M.G. Field, C.L. Decatur, M.J. Jager

Study supervision: J.W. Harbour

Grant Support

This work was supported by grants to J.W.H. from the National Cancer Institute (R01 CA125970 and CA161870), Research to Prevent Blindness, Inc. Senior Scientific Investigator Award, and Melanoma Research Alliance, to J.W.H. and M.G.F. from the Melanoma Research Foundation, to M.G.F. from the Sheila and David Fuente Graduate Program in Cancer Biology, Sylvester Comprehensive Cancer Center, to S.K. by the 2015 AACR-Ocular Melanoma Foundation Fellowship, in honor of Robert C. Allen, MD, Grant Number 15-40-39-KURT, and to the Bascom Palmer Eye Institute from NIH Core Grant P30EY014801, Research to Prevent Blindness Unrestricted Grant, and Department of Defense Grant #W81XWH-09-1-0675. The funding organizations had no role in the design or conduct of this research.

The costs of publication of this article were defrayed in part by the payment of page charges. This article must therefore be hereby marked *advertisement* in accordance with 18 U.S.C. Section 1734 solely to indicate this fact.

Received August 24, 2015; revised October 3, 2015; accepted October 23, 2015; published online March 1, 2016.

18. Krzywinski M, Schein J, Birol I, Connors J, Gascoyne R, Horsman D, et al. Circos: an information aesthetic for comparative genomics. *Genome Res* 2009;19:1639–45.
19. Harbour JW. A prognostic test to predict the risk of metastasis in uveal melanoma based on a 15-gene expression profile. *Methods Mol Biol* 2014;1102:427–40.
20. Onken MD, Worley LA, Person E, Char DH, Bowcock AM, Harbour JW. Loss of heterozygosity of chromosome 3 detected with single nucleotide polymorphisms is superior to monosomy 3 for predicting metastasis in uveal melanoma. *Clin Cancer Res* 2007;13:2923–7.
21. Costessi A, Mahrouf N, Tijchon E, Stunnenberg R, Stoel MA, Jansen PW, et al. The tumour antigen PRAME is a subunit of a Cul2 ubiquitin ligase and associates with active NFY promoters. *EMBO J* 2011;30:3786–98.
22. Aalto Y, Eriksson L, Seregard S, Larsson O, Knuutila S. Concomitant loss of chromosome 3 and whole arm losses and gains of chromosome 1, 6, or 8 in metastasizing primary uveal melanoma. *Invest Ophthalmol Vis Sci* 2001;42:313–7.
23. Ikeda H, Lethe B, Lehmann F, van Baren N, Baurain JF, de Smet C, et al. Characterization of an antigen that is recognized on a melanoma showing partial HLA loss by CTL expressing an NK inhibitory receptor. *Immunity* 1997;6:199–208.
24. Epping MT, Bernards R. A causal role for the human tumor antigen preferentially expressed antigen of melanoma in cancer. *Cancer Res* 2006;66:10639–42.
25. Clarke LE, Bryan Warf M, Flake DD 2nd, Hartman AR, Tahan S, Shea CR, et al. Clinical validation of a gene expression signature that differentiates benign nevi from malignant melanoma. *J Cutan Pathol* 2015;42:244–52.
26. Epping MT, Wang L, Edel MJ, Carlee L, Hernandez M, Bernards R. The human tumor antigen PRAME is a dominant repressor of retinoic acid receptor signaling. *Cell* 2005;122:835–47.
27. Crea F, Fornaro L, Bocci G, Sun L, Farrar WL, Falcone A, et al. EZH2 inhibition: targeting the crossroad of tumor invasion and angiogenesis. *Cancer Metastasis Rev* 2012;31:753–61.
28. Holling TM, Bergevoet MW, Wilson L, Van Eggermond MC, Schooten E, Steenbergen RD, et al. A role for EZH2 in silencing of IFN-gamma inducible MHC2TA transcription in uveal melanoma. *J Immunol* 2007;179:5317–25.
29. Epping MT, Wang L, Plumb JA, Lieb M, Gronemeyer H, Brown R, et al. A functional genetic screen identifies retinoic acid signaling as a target of histone deacetylase inhibitors. *Proc Natl Acad Sci U S A* 2007;104:17777–82.
30. Vertuani S, Dubrovskaya E, Levitsky V, Jager MJ, Kiessling R, Levitskaya J. Retinoic acid elicits cytostatic, cytotoxic and immunomodulatory effects on uveal melanoma cells. *Cancer Immunol Immunother* 2007;56:193–204.
31. Amir AL, van der Steen DM, van Loenen MM, Hagedoorn RS, de Boer R, Kester MD, et al. PRAME-specific Allo-HLA-restricted T cells with potent antitumor reactivity useful for therapeutic T-cell receptor gene transfer. *Clin Cancer Res* 2011;17:5615–25.
32. Nardini M, Gnesutta N, Donati G, Gatta R, Forni C, Fossati A, et al. Sequence-specific transcription factor NF-Y displays histone-like DNA binding and H2B-like ubiquitination. *Cell* 2013;152:132–43.
33. Silva AG, Graves HA, Guffei A, Ricca TI, Mortara RA, Jasiulionis MG, et al. Telomere-centromere-driven genomic instability contributes to karyotype evolution in a mouse model of melanoma. *Neoplasia (New York, NY)* 2010;12:11–9.
34. Kilic E, Koopmans AE, Yavuziyigitoglu S, Vaarwater J, van Ijcken WF, Paridaens D, et al. SF3B1 and EIF1AX mutations in uveal melanoma: a protective factor, or not? [abstract]. *Acta Ophthalmol [Abstracts from the 2014 European Association for Vision and Eye Research Conference]* 2014;92.
35. Midena E, de Belvis V, DeiTos AP, Antonini C. Isolated brain metastasis of malignant choroidal melanoma 27 years after enucleation. *Arch Ophthalmol* 1999;117:1553–6.